DALTON
FULL PAPER

Long-range chain orientation in 1-D co-ordination polymers as a function of anions and intermolecular aromatic interactions

Alexander J. Blake,[a] Gerhard Baum,[b] Neil R. Champness,*[a] Simon S. M. Chung,[a] Paul A. Cooke,[a] Dieter Fenske,[b] Andrei N. Khlobystov,[a] Dmitrii A. Lemenovskii,[c] Wan-Sheung Li[a] and Martin Schröder*[a]

[a] *School of Chemistry, The University of Nottingham, University Park, Nottingham, UK NG7 2RD*
[b] *Institut für Anorganische Chemie, Universität Karlsruhe, Engesserstr. Geb-Nr. 30.45, 76128 Karlsruhe, Germany*
[c] *Department of Chemistry, M.V.Lomonosov Moscow State University, Moscow, 119 899, Russia*

Received 1st August 2000, Accepted 6th October 2000
First published as an Advance Article on the web 16th November 2000

The influence of anions and intermolecular aromatic interactions on the orientation of one dimensional silver(I) co-ordination polymers has been studied. Reaction of AgX with 2,7-diazapyrene (diaz) (X = BF_4^- or NO_3^-), 1,4-bis(4-pyridyl)butadiyne (pybut) (X = BF_4^-, NO_3^-, PF_6^- or $MeCO_2^-$), 4,4′-bipy (X = BF_4^-) or 1,4-bis(4-pyridylethynyl)phenylene (pyphe) (X = PF_6^-) afforded products of general formula $\{[Ag(ligand)]X\}_\infty$. All of the products have been structurally characterised by single crystal X-ray diffraction confirming that they exist as one-dimensional linear chain co-ordination polymers. The arrangement of the chains with respect to each other in the solid state is discussed and evaluated in terms of the relative co-ordinating ability of the anion used and the tendency of the N-donor ligand to adopt intermolecular aromatic interactions. For the complexes of diaz the overriding force in controlling chain orientation was shown to be π–π interactions between diaz ligands on adjacent chains. In the case of the pybut complexes the most dominant forces were shown to be metal–anion interactions with aromatic π–π interactions and Ag · · · Ag interactions playing a less influential role. In the case of $\{[Ag(pyphe)]PF_6\}_\infty$ Ag · · · aromatic interactions are important in the overall arrangement of adjacent chains.

Introduction

The rapidly growing area of co-ordination polymers, polymeric compounds based on the interaction of metal cations with organic ligands, has given rise to a wide variety of fascinating one-, two- and three-dimensional structures. We now need to establish the general principles of the construction of such compounds according to their overall structure. Recent attempts at classification[1] help to highlight the relationship between the structure of the molecular building blocks and that of the supramolecular entity formed *via* self-assembly of those blocks. Understanding this relationship is the key to controlled design of supramolecular structures. Thus, many examples illustrating the factors that control the formation of co-ordination polymers have been recognised, including the functionality and denticity of ligands,[2] size and nature of anions[3] and/or solvent.[4] However, there are relatively few systematic studies on this subject.[2e,3b,4a]

The strategy for supramolecular design proposed by Desiraju[5] in 1995 is based on interpretation of crystal structures in terms of "supramolecular interactions" and "supramolecular synthons", allowing consideration of the structure of the "supermolecule" governed by superposition of discrete non-covalent intermolecular contacts. We report herein studies on Ag^I–bipyridyl co-ordination polymers and consider a number of supramolecular interactions that occur in this type of compound. These include intermolecular aromatic, Ag · · · Ag, Ag · · · aromatic and Ag · · · anion interactions and electrostatic repulsions (Scheme 1). Most information about these types of interactions has been obtained from studies on discrete molecular models designed to investigate the nature of specific "insulated" supramolecular interactions.[6] However, in a supramolecular array these intermolecular contacts combine so that the overall structure is a compromise between various interactions of different types and energies.[5] The exploitation of the synergic effects of one type of interaction upon another as part of supramolecular design is a critical challenge in crystal engineering. We illustrate herein how combinations of supramolecular interactions can affect the structure of 1-D chain-like co-ordination polymers which, due to their topological simplicity, may be used as models for investigating the influence of the different factors on the structure of the supramolecular entity.

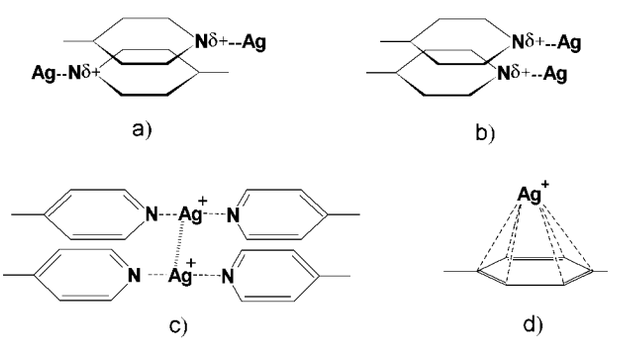

Scheme 1 Weak interactions observed in one-dimensional Ag^I–bipyridyl co-ordination polymers: (a) favourable head-to-tail aromatic π–π pyridyl–pyridyl interactions, (b) less-favourable head-to-head aromatic π–π pyridyl–pyridyl interactions, (c) Ag · · · Ag interactions, (d) Ag · · · aromatic interactions.

Results and discussion

Ligand structures

The discoid aromatic molecule diaz (2,7-diazapyrene) (Scheme 2) has 16 electrons in its delocalised π-electronic system.

DOI: 10.1039/b006202m

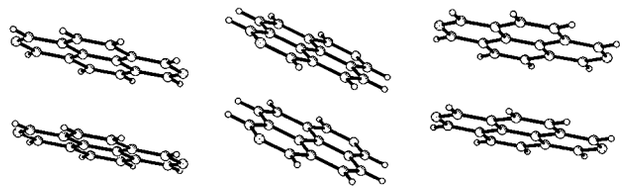

Fig. 1 Packing diagram of free diaz showing the "herringbone" arrangement of the molecules.

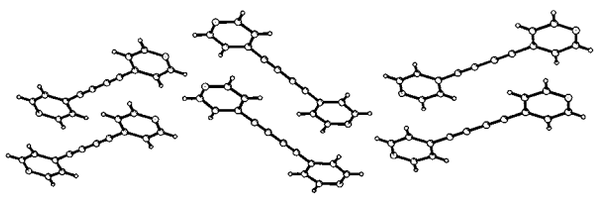

Fig. 2 Packing arrangement of free pybut showing the "herringbone" arrangement of the molecules.[10]

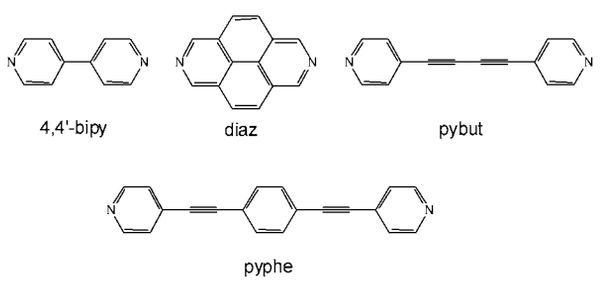

Scheme 2 Ligands used for constructing one-dimensional Ag^{I}–bipyridyl co-ordination polymers.

Aromatic molecules with such structures tend to interact *via* face-to-face stacking,[7] the driving force for their association being electrostatic attraction between aromatic π electrons and a positively charged ring σ framework.[8] The single crystal structure of the "free" ligand (Fig. 1) shows that this intermolecular interaction defines the packing arrangement with an interplanar separation between parallel molecules of 3.450(2) Å, and the centre of the molecules offset by 1.570(2) Å. The herringbone packing motif observed for diaz is common for aromatic compounds in the solid state.[5]

The structural isomer pybut [1,4-bis(4-pyridyl)butadiyne] has the same number of π electrons able to participate in intermolecular interactions but an alternative distribution of the electronic density within the molecule. The π electrons of the sp-hybridised carbons of the diyne linker are unlikely to take a significant part in any kind of intermolecular interaction in co-ordination polymers; thus, in contrast to the discoid ligand diaz, the groups prone to adoption of aromatic-based interactions are concentrated at the ends of the ligand. We can assume that the energy of the facial interaction increases proportionally with the number of π electrons in a fused aromatic system[9] and hence the energy of face-to-face aromatic interactions in pybut may be considered to be lower than for that observed for diaz. As a result of this lower energy the molecules of free pybut are packed less closely in the solid state with an interplanar separation of 3.523(5) Å and the centre of the molecules offset by 1.560(5) Å.[10] As with diaz, infinite aromatic stacks are organised in a herringbone motif (Fig. 2). As pybut and diaz differ in shape and electron distribution these two molecules confer different abilities to associate *via* aromatic interactions. Therefore, we expect the structures of supramolecular arrays formed by these ligands to differ because of the differences in the strength of π–π stacking.

Metal complex structures

Silver(I) complexes of *exo*-bidentate ligands often give rise to 1-D chain-like polymers because of the preference of Ag^{I} for a linear geometry.[11] The introduction of a metal centre to the structure may be considered as addition of a new non-covalent interaction into the supramolecular system.

Table 1 Selected interatomic distances [Å] and angles [°] for complexes **1**, **2**,[a] **3**,[b] **4**,[c] **5**,[d] **6**,[e] **7** and **9**[f]

Compound				
1	Ag1–N1	2.198(4)	N1–Ag1–N2	180
	Ag1–N2	2.203(4)		
2	Ag1–N1	2.215(4)	N1–Ag1–O1	93.98(13)
	Ag1–N1^{i}	2.215(4)	N1–Ag1–O1^{i}	119.1(2)
	Ag1–O1	2.547(4)	N1–Ag1–N1^{i}	144.2(2)
	Ag1–O1^{i}	2.547(4)	N1^{i}-Ag1–O1	119.1(2)
			N1^{i}-Ag1–O1^{i}	93.98(13)
			O1–Ag1–O1^{i}	50.5(2)
3	Ag1–N1	2.147(3)	N1–Ag1–N1^{i}	180
4	Ag1–N1	2.172(6)	N1–Ag1–N2^{i}	177.1(3)
	Ag1–N2^{i}	2.176(6)		
5	Ag1–N1	2.164(6)	N1–Ag1–N2^{i}	179.9(3)
	Ag1–N2^{i}	2.153(6)		
	Ag1–O1	2.687(6)		
6	Ag1–N1	2.185(3)	N1–Ag1–N2	169.88(10)
	Ag1–N2	2.186(3)	N1–Ag1–Ag1^{i}	97.04(8)
	Ag1 ··· Ag1^{i}	3.1927(10)	N2–Ag1–Ag1^{i}	92.96(8)
	Ag1–O1	2.636(3)		
	Ag1–O1^{i}	2.621(3)		
7	Ag1–N101	2.190(3)	N101–Ag1–N102	168.18(12)
	Ag1–N102	2.201(3)	N101–Ag1–Ag2	75.49(9)
	Ag1 ··· Ag2	3.1371(5)	N102–Ag1–Ag2	112.12(8)
	Ag1–O1	2.497(3)		
	Ag1–O2	2.746(3)		
9	Ag1–N1	2.152(3)	N1–Ag1–N2^{i}	177.28(12)
	Ag1–N2^{i}	2.149(3)		

[a] Symmetry operation i: $-x+\frac{3}{2}, -y+\frac{1}{2}, z$. [b] Symmetry operation i: $-x, -y+1, -z+1$. [c] Symmetry operation i: $x-1, y, z-1$. [d] Symmetry operation i: $x+1, y, z-1$. [e] Symmetry operation i: $-x+1, -y+1, -z+1$. [f] Symmetry operation i: $x+\frac{3}{2}, -y+\frac{1}{2}, z-\frac{1}{2}$.

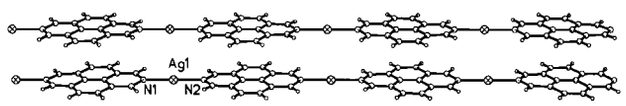

Fig. 3 Arrangement of infinite chains in $\{[Ag(diaz)]BF_4 \cdot MeCN\}_\infty$ **1**. Anions and solvent guest molecules are omitted for clarity (silver, cross-hatched).

Silver(I) complexes with 2,7-diazapyrene: control by facial π–π-interactions. The influence of Ag–N co-ordination interactions on the organisation of molecules in the crystal system is easily recognised as the relative orientation of the ligand molecules is changed from that observed for the "free" ligand. Thus, in complex **1** $\{[Ag(diaz)]BF_4 \cdot MeCN\}_\infty$ [1c] (Fig. 3) linear, coplanar ribbons of ligands are observed. It is clear that only a linear orientation of the ligand molecules, as observed in **1** (see Table 1) can meet the co-ordination requirements of two-co-ordinate Ag^{I}. Despite the reorientation of the diaz molecules, aromatic face-to-face contacts remain a dominant supramolecular interaction in complex **1**, with an interplanar separation between parallel diaz molecules of 3.380(5) Å (Fig. 3) compared to 3.450(2) Å in the "free" ligand. It is important to note that the co-ordination of diaz to the silver(I) cation strengthens the facial aromatic interaction due to an increase of both the positive charge of the σ framework and the π-electron density on the ligand, as a result of lone pair donation from the ligand nitrogen atoms and potential π back donation from the silver(I) cations. Such polarisation of the aromatic molecule encourages a more effective intermolecular interaction.[8] This π–π interaction results in a significant offset of the molecules [centre–centre separation = 3.640(5) Å, offset distance = 1.351(5) Å] and prevents close interaction of silver(I) cations [Ag ··· Ag 3.640(3) Å].[12] Indeed, the approach of

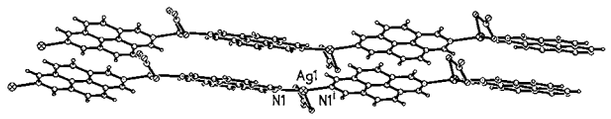

Fig. 4 Arrangement of infinite chains in $\{[Ag(diaz)(NO_3)]\}_\infty$ **2**. Symmetry code i: $-x+\frac{3}{2}$, $-y+\frac{1}{2}$, z (silver, cross-hatched; oxygen, right-hatched).

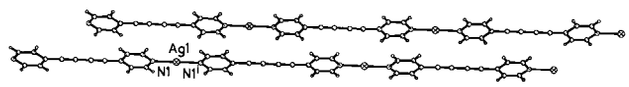

Fig. 5 Arrangement of infinite chains in $\{[Ag(pybut)]BF_4\cdot MeCN\}_\infty$ **3**. Anions and solvent guest molecules are omitted for clarity. Symmetry code i: $-x$, $-y+1$, $-z+1$ (silver, cross-hatched).

cationic centres in this case should be considered as a cause of repulsion between chains, with the Coulombic force counteracting the attractive aromatic stacking. Stacks of infinite polycationic chains form infinite sheets between which lie the BF_4^- anions (shortest Ag···F distance > 5 Å).

The crystal structure of $\{[Ag(diaz)(NO_3)]\}_\infty$ **2** supports this hypothesis (Fig. 4) as the chelating co-ordination of the NO_3^- anion to the Ag^I can be considered partially to neutralise the positive charge within the chain, allowing the interplanar separation to be reduced by 0.04 Å in comparison to that of complex **1** [interplanar separation = 3.340(5) Å, centre–centre separation = 3.749(5) Å, offset distance = 1.703(5) Å]. As a result of NO_3^- co-ordination, Ag^I adopts a strongly distorted tetrahedral geometry with a N1–Ag–N1^i angle of 144.2(2)°, with the linearity observed in compound **1** altered in polymer **2** into zigzag shaped chains where neighbouring ligand molecules are twisted with respect to each other by 17.6(2)°. In this way the packing arrangement of diaz molecules in **2** resembles the herringbone motif observed in the "free" ligand. The structures of complexes **1** and **2** demonstrate that co-ordination of Ag^I to diaz does not preclude face-to-face aromatic interactions; indeed these are the strongest intermolecular contacts in structures containing diaz, thus preventing formation of a polymer with a "shifted" placement of chains (Scheme 3). Therefore,

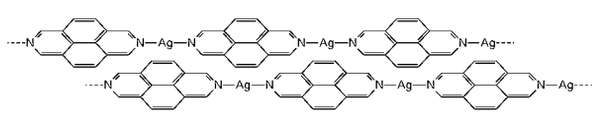

Scheme 3 Possible "shifted" placement of chains that is overcome by the adoption of π–π interactions adopted by the diaz ligands.

the relatively weak potential interactions between Ag^I and π electrons cannot compensate for the loss of the stronger face-to-face aromatic contacts.

Silver complexes with 1,4-bis(4-pyridyl)butadiyne: control by synergic π–π, Ag–Ag and Ag–anion interactions. As previously noted, the rod-like ligand pybut (Scheme 2) exhibits weaker π–π interactions than does diaz allowing alternative arrangements of linear chains. For example, the complex $\{[Ag(pybut)]BF_4\cdot MeCN\}_\infty$ **3** (Fig. 5) consists of chains arranged in a parallel fashion, where the ligand molecules are shifted relative to each other so that the shortest interchain Ag···Ag distance is 7.147(4) Å. Again the herringbone packing of the free ligand is disrupted by silver(I) co-ordination. This shifted type of placement can be accounted for by Coulombic repulsions between silver(I) centres, and in this case the repulsion is not compensated by face-to-face ligand stacking in contrast to $\{[Ag(diaz)]BF_4\}_\infty$ **1**. Nevertheless, the aromatic groups in **3** are involved in face-to-face interactions in a "head-to-tail" fashion with an interplanar separation of 3.536(6) Å (Scheme 1a). This arrangement is energetically more favourable than a "head-to-head" orientation (Scheme 1b), due to more effective charge

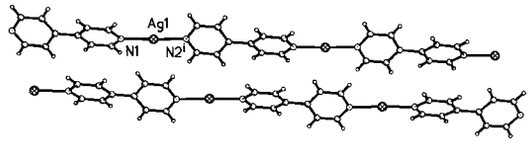

Fig. 6 Arrangement of infinite chains in $\{[Ag(4,4'\text{-bipy})]BF_4\cdot H_2O\cdot MeCN\}_\infty$ **4**. Anions and solvent guest molecules are omitted for clarity. Symmetry code i: $x-1$, y, $z-1$ (silver, cross-hatched).

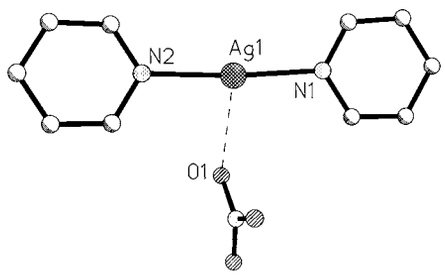

Fig. 7 Co-ordination geometry of Ag^I in $\{[Ag(pybut)]NO_3\cdot MeCN\}_\infty$ **5**. Hydrogen atoms are omitted for clarity (silver, cross-hatched; oxygen, right-hatched; nitrogen, dotted).

separation. As the BF_4^- anions are unco-ordinated, and located between the aromatic stacks, the metal centres have a perfect linear geometry (Table 1). It should be noted that the related bipyridyl ligand 4,4′-bipy (Scheme 2) gives the complex $\{[Ag(4,4'\text{-bipy})]BF_4\cdot H_2O\cdot MeCN\}_\infty$ **4** which exhibits essentially the same packing motif, and where the cationic repulsion is minimised with the same "head-to-tail" aromatic pairing (Fig. 6). The shortest interplanar separation is 3.456(6) Å and the shortest interchain Ag···Ag distance is 5.838(3) Å. A recently published account of π–π stacking in metal complexes which demonstrates that "head-to-tail" stacking is more common is supported by numerous examples of co-ordination compounds.[8c] Although water is included in the structure of **4** it is not involved in any hydrogen bonding and therefore does not appear to play a significant role in the overall packing arrangement.

The structure of the complex $\{[Ag(pybut)]NO_3\cdot MeCN\}_\infty$ **5** demonstrates the same "head-to-tail" structural pattern observed in complex **3**. Once again weak co-ordination of the anions (Fig. 7) causes the cationic centres to be closer than in **3**, with a Ag···Ag separation of 7.079(2) Å observed for **5**.

Bidentate anions, such as $PO_2F_2^-$ and $MeCO_2^-$, have a higher density of negative charge on their peripheral, potentially interacting, atoms than NO_3^- or BF_4^-: they are therefore able to co-ordinate more strongly and can significantly mediate other interchain interactions. Thus, in the case of the complex $\{[Ag(pybut)]PO_2F_2\cdot MeCN\}_\infty$ **6** each silver(I) cation interacts weakly with two $PO_2F_2^-$ anions with Ag–O distances of 2.636(3) and 2.621(3) Å, allowing the cations to be closer and therefore form Ag···Ag interactions at a distance 3.1927(10) Å. Weak asymmetric bridging of silver(I) cations by two oxygen donors (Fig. 8) may also enhance the interchain contact. In addition to these Ag···Ag and Ag–anion interactions, the structure of **6** also contains "head-to-head" aromatic interactions characterised by an interplanar separation of 3.394(3) Å which bind adjacent chains together to afford infinite "ladders" (Fig. 9) in which the silver(I) centres adopt a T-shaped co-ordination geometry (Table 1). A comparison of complexes **3** and **6** allows us to attribute their structural differences exclusively to the different co-ordinative abilities of BF_4^- and $PO_2F_2^-$ anions, as both anions have a similar size and tetrahedral shape, and the complexes were prepared under the same conditions (MeCN, 70 °C). The tetrahedral anion $PO_2F_2^-$ may therefore be considered a more co-ordinating analogue of BF_4^-.

Similarly to the relationship between $PO_2F_2^-$ and BF_4^-, acetate can be related to the trigonal NO_3^- anion. Thus, the

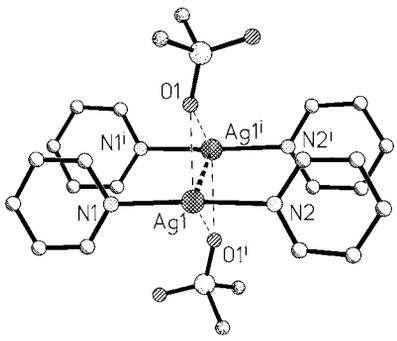

Fig. 8 Co-ordination geometry of Ag^{I} in $\{[Ag(pybut)]PO_2F_2\cdot MeCN\}_\infty$ **6**. Symmetry code i: $-x+1$; $-y+1$; $-z+1$. Hydrogen atoms are omitted for clarity (silver, cross-hatched; oxygen, right-hatched; nitrogen, dotted; phosphorus, light random dot pattern; fluorine, heavy random dot pattern).

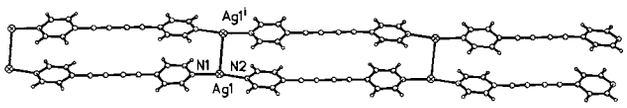

Fig. 9 Arrangement of infinite chains in $\{[Ag(pybut)]PO_2F_2\cdot MeCN\}_\infty$ **6**. Anions and solvent guest molecules are omitted for clarity. Symmetry code i: $-x+1$, $-y+1$, $-z+1$ (silver, cross-hatched).

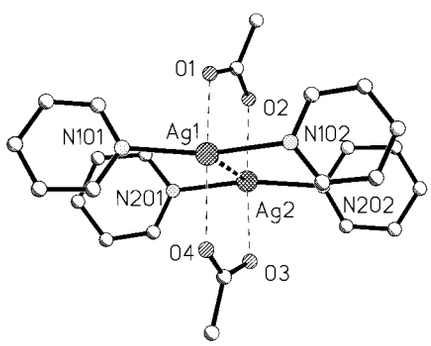

Fig. 10 Co-ordination geometry of Ag^{I} in $\{[Ag(pybut)]MeCO_2\cdot 2.5H_2O\}_\infty$ **7**. Hydrogen atoms are omitted for clarity (silver, cross-hatched; oxygen, right-hatched; nitrogen, dotted).

acetate anion can effectively neutralise cationic positive charge and is able to bridge cations in $\{[Ag(pybut)]MeCO_2\cdot 2.5H_2O\}_\infty$ **7** (Fig. 10), with a Ag···Ag separation of 3.1371(5) Å, which results in the same "head-to-head" ligand arrangement as observed in complex **6**.

Silver complex with 1,4-bis(4-pyridylethynyl)phenylene: control by Ag–aromatic interaction. The interaction between cations and the π-electron system of a ligand represents another possible driving force for supramolecular structure formation.[13] There are about 130 examples of Ag–η^1- and Ag–η^2-arene bonding found in the Cambridge Structural Database with a mean Ag–arene distance of 2.82 Å.[14] Structural statistics on long range Ag–η^6 interactions are less reliable (Scheme 1d), but the importance of such interactions has previously been demonstrated in the significant work of Hosseini and co-workers.[13c] Despite the long range interaction and its relative weakness, Ag–η^6 contacts with arenes have been documented in the solid state, including the first example of an arene–Ag sandwich compound;[14] the same work summarises structural statistics for metal–η^6 species and reports a range of Ag–centroid distances of 2.89–3.37 Å.[14]

The ligand pyphe [1,4-bis(4-pyridylethynyl)phenylene] can be considered as an elongated version of pybut (Scheme 2) where the *p*-phenylene group separates the two C≡C bonds and provides a maximum potential for aromatic-based interactions at the midpoint of the ligand. In the presence of co-ordinating anions (*e.g.* $PO_2F_2^-$, NO_3^-) it is likely that structures of

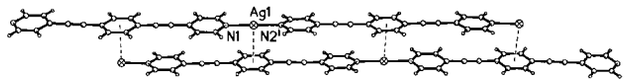

Fig. 11 Arrangement of infinite chains in $\{[Ag(pyphe)]PF_6\cdot MeCN\}_\infty$ **9**. Ag···aromatic interactions represented by dotted lines. Anions and solvent guest molecules are omitted for clarity. Symmetry code i: $x+\frac{3}{2}$, $-y+\frac{1}{2}$, $z-\frac{1}{2}$ (silver, cross-hatched).

complexes with pyphe could be very similar to their pybut analogues, with the role of the co-ordinating anion dominating over weaker supramolecular forces. Although $\{[Ag(pyphe)]NO_3\cdot\}_\infty$ **8** could be isolated as a microcrystalline solid we were unable to obtain crystals of sufficient quality for single crystal X-ray diffraction analysis. However, we were interested to assess the impact of these weaker aromatic interactions and therefore prepared the linear silver(I) cationic polymer in the presence of less-co-ordinating PF_6^- anions. Thus in the absence of Ag^{I}–anion contacts the chains adopt a different stacking motif from that observed in $\{[Ag(pybut)]BF_4\cdot MeCN\}_\infty$ **3** and $\{[Ag(4,4'\text{-bipy})]BF_4\cdot H_2O\cdot MeCN\}_\infty$ **4**. In $\{[Ag(pyphe)]PF_6\cdot MeCN\}_\infty$ **9** the silver(I) centres have distorted linear co-ordination geometries (Table 1), with the chains significantly shifted with respect to each other [shortest Ag···Ag distance 5.177(3) Å; Fig. 11]. This again can be considered as an effect of the electrostatic repulsion of the cations. However, a more detailed analysis of the structure of complex **9** reveals only one type of attractive interaction between adjacent chains, namely the Ag···phenylene contact with a Ag···plane distance of 3.273(3) Å. This interaction therefore defines the overall packing arrangement.

Related 1-D silver complexes with pyridyl-donor ligands. The co-ordination sphere of Ag^{I} is very flexible and can adopt co-ordination numbers between 2 and 6 and various geometries from linear through to tetrahedral, trigonal pyramidal and octahedral.[15] This gives rise to a wide variety of 1-, 2- and 3-dimensional complexes based on silver(I) cations co-ordinated to bridging bipyridyl ligands.[16] The silver(I) cation usually prefers a linear, two co-ordinate geometry with nitrogen donors,[11] thus encouraging the formation of 1-D polymers with bridging bidentate ligands. However, the number of studies of the influence of anions on a given silver(I) system in 1-D polymers is limited.

Some examples relevant to our research have been reported for 1-D complexes of the smallest aromatic bidentate pyridyl-type ligand pyrazine (pyz). Both complexes $\{[Ag(pyz)][PF_6]_{0.5}[OH]_{0.5}\}_\infty$[16b] and $\{[Ag(pyz)]BF_4\}_\infty$[16a] with non-co-ordinating anions exhibit the same structural motif as that of $\{[Ag(diaz)]BF_4\}_\infty$. The ligand molecules are involved in aromatic intermolecular interactions (plane to plane separation 3.56 and 3.66 Å, respectively) but the chains are not sufficiently close for Ag···Ag interactions to be adopted (separations are 3.57 and 4.28 Å, respectively). The influence of the more co-ordinating NO_3^- anion is essentially the same as observed for diaz complexes: it distorts the linear geometry of silver(I) centres and allows adjacent chains to be closer[17] (Ag···Ag distance 3.560 Å, plane to plane separation 3.436 Å). It can also be deduced that pyrazine molecules, with a relatively small aromatic π-electronic system, can tolerate complete loss of aromatic interactions if they are compensated by another supramolecular contact. For example, in the 1-D complex $\{[Ag(pyz)(NO_2)]\}_\infty$ no aromatic interactions are observed between chains, rather the chain arrangement is defined by moderate Ag···Ag interactions [3.2168(3) Å].[18] 4,4′-Bipyridyl has been found to be more structurally flexible than pybut in silver(I) co-ordination polymers. Thus in $\{[Ag(4,4'\text{-bipy})]NO_3\}_\infty$ the NO_3^- anion is weakly co-ordinating [Ag···O 2.790(2) Å] and the orthogonal linear chains are linked *via* Ag···Ag contacts.[12a,d] This contrasts with both the structure of $\{[Ag(4,4'\text{-bipy})]BF_4\cdot H_2O\}_\infty$ and with the other structural

motifs that we have observed with other complexes of $AgNO_3$ and linear bipyridyl ligands. The unique structural features of $\{[Ag(4,4'\text{-bipy})]NO_3\}_\infty$ are a result of a combination of two non-conflicting interchain interactions. Coplanar pyridyl rings stack (plane to plane separation 3.522 Å) and are twisted by 90° with respect to each other (which allows an effective charge separation) and the Ag(I) cations form short Ag···Ag contacts [2.970(2) Å]. This remarkable structure is perhaps a consequence of the specific geometry of 4,4′-bipy which fits this particular packing arrangement of chains; however, a direct comparison of this structure with other complexes is difficult because $\{[Ag(4,4'\text{-bipy})]NO_3\}_\infty$ was synthesized under unusual conditions (water, 140 °C) differing considerably from those applied for the syntheses of most 1-D silver(I) polymers. $\{[Ag(4,4'\text{-bipy})]NO_2\}_\infty$, in which the NO_2^- anion co-ordinates at a similar distance (Ag···O 2.667 Å)[18] as the NO_3^- anion in $\{[Ag(pybut)]NO_3\}_\infty$ (Ag···O 2.687 Å), adopts the same chain as observed for $\{[Ag(4,4'\text{-bipy})]BF_4\cdot H_2O\}_\infty$ ("head-to-tail" stacking of pyridyl rings, plane-to-plane separation 3.383 Å) as would be expected considering the charge compensation afforded by the anionic interaction.

Conclusion

Comparison between the crystal structures of "free" ligands and those of their complexes allows interpretation of the influence of metal cation co-ordination on the effectiveness of aromatic face-to-face interactions within a polymeric array. Varying the anion within the supramolecular complex reveals its role in determining the overall interactions between chains. The isomeric bipyridyl ligands diaz and pybut have very different π-electron distributions: the discoid shape of diaz consistently favours intermolecular aromatic π–π face-to-face interactions. Moreover, the interplanar separations of diaz molecules may be fine-tuned by controlling metal–anion interactions.

The elongated pybut ligand provides structural flexibility in its complexes. The relative placement of the ligand molecules and the orientation of the infinite cationic chains can be varied by metal–anion interactions, co-ordinating anions allowing closer approaches between cationic centres and the formation of "head-to-head" ligand placement as seen in complexes **6** and **7**. In the case of relatively weakly co-ordinating anions (BF_4^-, NO_3^-) the polymer adopts an alternative chain arrangement where ligands have a "head-to-tail" orientation and the cationic centres are separated by over 7 Å as observed in **4** and **5**.

Using rod-like ligands, which include π-electron donating units (phenylene ring) in their spacers, allows exploitation of Ag···aromatic interactions when combined with a non-co-ordinating anion, as exemplified by complex **9**.

We believe that by interpreting the structures of co-ordination polymers in terms of the relative energies and directionality of weak supramolecular interactions a greater appreciation of co-ordination polymer design can be achieved. We are now extending this approach to supramolecular structures with higher dimensionality and topological complexity.

Experimental

All reagents (Aldrich) were used as received. Ligands pybut and pyphe were prepared by literature methods.[19,20] The synthesis of diaz[21] was modified from the reported procedure. Elemental analyses were carried out by the University of Nottingham microanalysis service. Infrared spectra were obtained as KBr pressed pellets using a Perkin-Elmer 1600 series FTIR spectrometer.

Syntheses

Diaz. 1,3,6,8-Tetrahydro-2,7-dimethyl-2,7-diazapyrene (2.4 g, 1×10^{-2} mol) prepared by the literature method[22] was thoroughly mixed with powdered grey selenium metal (4.8 g, 6×10^{-2} mol). The mixture was placed in a 20 cm^3 flask fitted with a gas exhaust tube then heated in a sand bath at 265 °C for 3 h. The temperature was increased to 300–310 °C for 1 h. The product was sublimed and deposited onto the cold neck of the reaction vessel as yellow acicular crystals. It was removed and recrystallised from benzene. Sublimation of the product under reduced pressure (14 mmHg) gave 1.62 g yellow crystals of pure diaz (yield 82%). NMR, IR and elemental analysis are identical to the previously reported values.[21]

$\{[Ag(diaz)(NO_3)]\}_\infty$ 2. A solution of $AgNO_3$ (13 mg, 7.4×10^{-2} mmol) in MeCN (2 cm^3) was layered over a solution of diaz (15 mg, 7.4×10^{-2} mmol) in benzonitrile (2 cm^3). After 5 days large colourless crystals suitable for X-ray diffraction were formed (yield 20 mg, 73%). IR, ν/cm^{-1}: 3052m, 2923w, 2852m, 1588w, 1578w, 1384vs, 1315s, 1149w, 1121w, 1035w, 905m, 831w, 791w and 713m. Calc. for $C_{14}H_8AgN_3O_3$: C 44.92, H 2.14, N 11.23. Found: C 44.57, H 2.03, N 11.30%.

$\{[Ag(pybut)]BF_4\cdot MeCN\}_\infty$ 3. A solution of $AgBF_4$ (20 mg, 9.8×10^{-2} mmol) in MeCN (2 cm^3) was added to a solution of pybut (20 mg, 9.8×10^{-2} mmol) in MeCN (2 cm^3) at 70 °C (external temperature, oil bath). The resulting solution was heated at 70 °C for 1 h. The temperature was then slowly decreased to 20 °C over 10 h. Colourless crystals suitable for X-ray diffraction were formed (24 mg). An additional amount of complex **3** (11 mg) was precipitated by diethyl ether diffusion into the reaction solution. Overall yield 80%. Complex **3** readily loses solvent and can be completely desolvated *in vacuo*. IR, ν/cm^{-1}: 3027w, 1940w, 1585vs, 1539w, 1486w, 1399m, 1125–1036vs, 814vs, 779m and 542s. Calc. for $C_{14}H_8AgBF_4N_2$ (desolvated complex): C 42.40, H 2.36, N 7.60. Found: C 42.10, H 2.01, N 7.12%.

$\{[Ag(4,4'\text{-bipy})]BF_4\cdot H_2O\cdot MeCN\}_\infty$ 4. The same method as for complex **3**, using $AgBF_4$ (19 mg, 9.6×10^{-2} mmol) and 4,4′-bipy (15 mg, 9.6×10^{-2} mmol), gave colourless crystals (yield 34 mg, 87%). Complex **4** readily loses solvent and can be completely desolvated *in vacuo*. IR, ν/cm^{-1}: 3439w, 3052w, 1599s, 1532w, 1423w, 1406w, 1220w, 1070–1034vs, 805s, 627w and 533w. Calc. for $C_{10}H_8AgBF_4N_2$ (desolvated complex): C 34.19, H 2.28, N 7.98. Found: C 33.85, H 2.02, N 7.79%.

$\{[Ag(pybut)]NO_3\cdot MeCN\}_\infty$ 5. The same method as for complex **3**, using $AgNO_3$ (17 mg, 9.8×10^{-2} mmol) and pybut (20 mg, 9.8×10^{-2} mmol), gave colourless crystals (yield 31 mg, 77%). Complex **5** readily loses solvent and can be completely desolvated *in vacuo*. IR cm^{-1}: 3048w, 2250w, 1939w, 1584s, 1538m, 1486w, 1385vs, 1270w, 1062w, 825w, 814s, 778m, 541m and 460m. Calc. for $C_{14}H_8AgN_3O_3$ (desolvated complex): C 44.65, H 2.13, N 11.24. Found: C 44.91, H 2.01, N 11.23%.

$\{[Ag(pybut)]PO_2F_2\cdot MeCN\}_\infty$ 6. The same method as for complex **3**, using $AgPF_6$ (25 mg, 9.8×10^{-2} mmol) and pybut (20 mg, 9.8×10^{-2} mmol), gave colourless crystals (yield 24 mg, 55%). Anion PF_6^- was found to be hydrolysed to $PO_2F_2^-$. IR, ν/cm^{-1}: 3026w, 2922w, 1939w, 1584s, 1539w, 1486w, 1398m, 1332m, 1314s, 1153s, 852m, 836m, 814s, 779m, 542m, 513m and 498m. Calc. for $C_{16}H_{11}AgF_2N_3O_2P$: C 42.28, H 2.42, N 9.25. Found: C 41.95, H 2.40, N 8.93%.

$\{[Ag(pybut)]MeCO_2\cdot 2.5H_2O\}_\infty$ 7. A solution of $AgMeCO_2$ (10 mg, 6.0×10^{-2} mmol) in a 1 : 1 mixture of water and MeCN (2 cm^3) was layered over a solution of pybut (12 mg, 6.0×10^{-2} mmol) in benzonitrile (2 cm^3). Colourless crystals were obtained (yield 15 mg, 67%). The product readily loses solvent and can be completely desolvated *in vacuo*. IR, ν/cm^{-1}: 3404m, 1940w, 1585s, 1557s, 1539m, 1486w, 1411s, 1405s, 815s, 779m, 650w and 542m. Calc. for $C_{16}H_{11}AgN_2O_2$ (desolvated

Table 2 Crystal data and collection parameters for diaz and compounds **2**–**7**, **9**

	diaz	**2**	**3**	**4**	**5**	**6**	**7**	**9**
Empirical formula	$C_{14}H_8N_2$	$C_{28}H_{16}Ag_2N_6O_6$	$C_{16}H_{11}AgBF_4N_3$	$C_{12}H_{13}AgBF_4N_3O$	$C_{16}H_{11}AgN_4O_3$	$C_{16}H_{11}AgF_2N_3O_2P$	$C_{17.7}H_{19.18}AgN_2O_{4.92}$	$C_{22}H_{15}AgF_6N_3P$
M	204.22	748.21	439.96	409.93	415.16	454.12	440.03	574.21
Crystal system	Monoclinic	Orthorhombic	Monoclinic	Triclinic	Monoclinic	Triclinic	Triclinic	Monoclinic
Space group	$P2_1/c$	*Pccn*	*P*2/*c*	$P\bar{1}$	*P*2/*c*	$P\bar{1}$	$P\bar{1}$	*C*2/*c*
a/Å	3.7891(12)	18.4700(10)	8.175(3)	7.273(2)	7.134(2)	7.4930(15)	13.864(3)	9.263(2)
b/Å	8.0997(16)	3.748(12)	7.147(2)	10.506(3)	7.322(2)	8.2850(17)	14.110(3)	18.543(4)
c/Å	15.421(4)	16.667(5)	14.917(4)	10.642(3)	31.725(4)	14.723(3)	15.895(3)	30.160(6)
α/°				96.33(4)		101.91(3)	82.28(3)	
β/°	93.96(3)	90	91.28(3)	103.29(3)	97.53(2)	90.11(3)	89.34(3)	91.93(3)
γ/°				98.16(3)		107.69(3)	72.36(3)	
U/Å^3	472.1(2)	1154(4)	871.3(5)	774.7(4)	1642.8(5)	850.0(3)	2934.9(10)	5177.5(18)
Z	2	2	2	2	4	2	6	8
T/K	150(2)	150(2)	298(2)	220(2)	150(2)	293(2)	150(2)	193(2)
μ/mm^{-1}	0.087	1.762	1.199	1.345	1.240	1.315	1.045	1.473
Reflections collected	2590	3914	2352	3981	3475	4703	29777	13505
Unique reflections (R_{int})	839 (0.017)	904 (0.062)	1534 (0.050)	2730 (0.047)	3211 (0.077)	3005 (0.025)	13436 (0.025)	5723 (0.049)
Final *R*1 [$F > 4\sigma(F)$]	0.0366	0.0293	0.0456	0.0640	0.0882	0.0308	0.0413	0.0577
*w*R2 (all data)	0.900	0.0731	0.1115	0.1528	0.2331	0.0718	0.1101	0.0711

complex): C 51.75, H 2.96, N 7.55. Found: C 51.55, H 2.89, N 7.13%.

{[Ag(pyphe)]NO_3·MeCN}$_\infty$ 8. A solution of $AgNO_3$ (7.5 mg, 3.6×10^{-2} mmol) in MeCN (2 cm^3) was added to a solution of pyphe (10 mg, 3.6×10^{-2} mmol) in benzonitrile (2 cm^3). Slow diffusion of diethyl ether into the resulting solution gave a colourless polycrystalline precipitate (yield 14 mg, 84%). Using different conditions (*e.g.* MeCN/70 °C) resulted in the same polycrystalline material. The product readily loses solvent and can be completely desolvated *in vacuo*. IR, *ν*/cm^{-1}: 3082w, 3050w, 2221m, 1584s, 1535w, 1514m, 1403m, 1385s, 1213m, 813s, 627m, 561m and 539m. Calc. for $C_{20}H_{12}AgN_3O$ (desolvated complex): C 57.44, H 2.89, N 10.05. Found: C 56.98, H 2.36, N 9.68%.

{[Ag(pyphe)]PF_6·MeCN}$_\infty$ 9. A solution of $AgPF_6$ (9 mg, 3.6×10^{-2} mmol) in MeCN (2 cm^3) was added to a solution of pyphe (10 mg, 3.6×10^{-2} mmol) in benzonitrile (2 cm^3). Slow diffusion of diethyl ether into the resulting solution gave colourless crystals (yield 10 mg, 48%). The product readily loses solvent and can be completely desolvated *in vacuo*. IR, *ν*/cm^{-1}: 3080w, 3050w, 2221m, 1589s, 1538w, 1515m, 1407m, 1213m, 838vs, 627m, 561m and 539m. Calc. for $C_{20}H_{12}AgF_6N_2P$ (desolvated complex): C 44.64, H 2.08, N 5.65. Found: C 44.93, H 2.25, N 5.24%.

X-Ray crystallography

Single crystal X-ray experiments were performed on a Stoe Stadi-4 four circle diffractometer equipped with an Oxford Cryosystems open flow cryostat[23] for diaz and complexes **3**–**6**, an Enraf-Nonius FAST TV detector diffractometer for **2**, a Stoe IPDS image plate diffractometer for **9** and a Bruker SMART CCD area detector diffractometer for **7**, all collections used graphite Mo-Kα radiation $\lambda = 0.71073$ Å. Absorption corrections were performed by Gaussian Integration following refinement of the crystal morphology and dimensions against a set of ψ scans (**4** and **6**) or numerical methods (**3** and **5**). All structures were solved using direct methods using SHELXS 97[24] and all non-hydrogen atoms located using subsequent Fourier difference methods.[25] In all cases hydrogen atoms were placed in calculated positions and thereafter allowed to ride on their parent atoms; hydrogen atoms of acetonitrile guest molecules in complexes **4**, **5**, **6** and **9** were located from ΔF syntheses; in **3** hydrogen atoms of acetonitrile were not found because of disorder of the guest molecule. The disordered bonds in the disordered BF_4^- anion in **4** were restrained to have equal length. Compound **3** exhibited a disorder of one B–F bond modelled over two equally occupied sites. Structure **7** has 10.5 water molecules and 7 disordered molecules of MeOH per unit cell. Their hydrogen atoms were not found due to the high degree of disorder in the solvent-filled region of the structure. Crystal data for the compounds are listed in Table 2.

CCDC reference number 186/2218.

See http://www.rsc.org/suppdata/dt/b0/b006202m/ for crystallographic files in .cif format.

References

1 (*a*) R. Robson and S. Batten, *Angew. Chem., Int. Ed.*, 1998, **37**, 1460; (*b*) P. J. Hagrman, D. Hagrman and J. Zubieta, *Angew. Chem., Int. Ed.*, 1999, **38**, 2638; (*c*) A. J. Blake, N. R. Champness, P. Hubberstey, W.-S. Li, M. A. Withersby and M. Schröder, *Coord. Chem. Rev.*, 1999, **183**, 117.

2 For examples of control by ligand functionality see: (*a*) L. R. MacGillivary, S. Subramanian and M. J. Zaworotko, *J. Chem. Soc., Chem. Commun.*, 1994, 1325; (*b*) A. J. Blake, N. R. Champness, S. S. M. Chung, W.-S. Li and M. Schröder, *Chem. Commun.*, 1997, 1005; (*c*) A. J. Blake, N. R. Champness, A. N. Khlobystov, D. A. Lemenovskii, W.-S. Li and M. Schröder, *Chem. Commun.*, 1997,

1339; (*d*) M. Fujita, Y. J. Kwon, O. Sasaki, K. Yamaguchi and K. Ogura, *J. Am. Chem. Soc.*, 1995, **117**, 7287; (*e*) Y.-H. Kiang, G. B. Gardner, S. Lee, Z. Xu and E. B. Lobkovsky, *J. Am. Chem. Soc.*, 1999, **121**, 8204; (*f*) A. J. Blake, N. R. Champness, P. A. Cooke, J. E. B. Nicolson and C. Wilson, *J. Chem. Soc.*, *Dalton Trans.*, 2000, 3811.

3 For examples of anion control see: (*a*) M. A. Withersby, A. J. Blake, N. R. Champness, P. Hubberstey, W.-S. Li and M. Schröder, *Angew. Chem.*, *Int. Ed. Engl.*, 1997, **36**, 2327; (*b*) K. A. Hirsch, S. R. Wilson and J. S. Moore, *Inorg. Chem.*, 1997, **36**, 2960.

4 For examples of solvent control see: (*a*) M. A. Withersby, A. J. Blake, N. R. Champness, P. A. Cooke, P. Hubberstey, W.-S. Li and M. Schröder, *Inorg. Chem.*, 1999, **38**, 2259; (*b*) S. Subramanian and M. J. Zaworotko, *Angew. Chem.*, *Int. Ed. Engl.*, 1995, **34**, 2127; (*c*) R. W. Gable, B. F. Hoskins and R. Robson, *J. Chem. Soc.*, *Chem. Commun.*, 1990, 1677; (*d*) J. Lu, T. Paliwala, S. C. Lim, C. Yu, T. Niu and A. J. Jacobson, *Inorg. Chem.*, 1997, **36**, 923.

5 G. R. Desiraju, *Angew. Chem.*, *Int. Ed. Engl.*, 1995, **34**, 2311.

6 For examples of π–π interaction see: J. Zhang and J. S. Moore, *J. Am. Chem. Soc.*, 1992, **114**, 9701; S. Paliwal, S. Geib and C. S. Wilcox, 1994, **116**, 4497; H. Adams, F. J. Carrer, C. A. Hunter, J. S. Morales and E. M. Seward, *Angew. Chem.*, *Int. Ed. Engl.*, 1996, **35**, 1542. Ag–Ag interaction: P. Pyykko, *Chem. Rev.*, 1997, 597 and references therein. Ag–aromatic interaction: J. N. H. Raek, H. Engelkamp, A. E. Rowan, J. A. A. W. Elemans and R. J. M. Nolte, *Chem. Eur. J.*, 1998, **4**, 716; (*f*) N. Yanagihara and T. Gotoh, *Polyhedron*, 1996, **15**, 4349.

7 R. Kiralj, B. Kojic-Prodic, I. Piantanida and M. Zinic, *Acta Crystallogr.*, *Sect. B*, 1999, **55**, 55.

8 (*a*) C. A. Hunter and J. K. Sanders, *J. Am. Chem. Soc.*, 1990, **112**, 5525; (*b*) C. A. Hunter, *Chem. Soc. Rev.*, 1994, 101; (*c*) C. Janiak, *J. Chem. Soc.*, *Dalton Trans.*, 2000, 3885.

9 J. Dunitz and A. Gavezzotti, *Acc. Chem. Res.*, 1999, **32**, 677.

10 J. R. Allan, M. J. Barrow, P. C. Beaumont, L. A. Macindoe, G. H. W. Milburn and A. R. Werninck, *Inorg. Chim. Acta*, 1988, **148**, 85.

11 *Comprehensive Co-ordination Chemistry*, ed. G. Wilkinson, Pergamon, Oxford, 1987, vol. 2, p. 74.

12 For examples of unsupported Ag···Ag interactions see: (*a*) F. Robinson and M. J. Zaworotko, *J. Chem. Soc.*, *Chem. Commun.*, 1995, 2413; (*b*) M.-L. Tong, X.-M. Chen, B.-H. Ye and L.-N. Ji, *Angew. Chem.*, *Int. Ed.*, 1999, **38**, 2237; (*c*) C. N. R. Rao, A. Rauganathan, V. R. Pedireddi and A. J. Raju, *Chem. Commun.*, 2000, 39; (*d*) O. M. Yaghi and H. Li, *J. Am. Chem. Soc.*, 1996, **118**, 295.

13 (*a*) M. Munakata, L. P. Wu, T. Kuroda-Sowa, M. Maekawa, Y. Suenaga, G. L. Ning and T. Kojima, *J. Am. Chem. Soc.*, 1998, **120**, 8610; (*b*) G. L. Ning, L. P. Wu, K. Sugimoto, M. Munakata, T. Kuroda-Sowa and M. Maekawa, *J. Chem. Soc.*, *Dalton Trans.*, 1999, 2529; (*c*) R. Sneider, M. W. Hosseini, J.-M. Planeix, A. D. Cian and J. Fischer, *Chem. Commun.*, 1998, 1625.

14 M. Mascal, J. L. Kerdelhue, A. J. Blake, P. A. Cooke, R. J. Mortimer and S. J. Teat, *Eur. J. Inorg. Chem.*, 2000, 485.

15 D. Venkataraman, Y. Du, S. R. Wilson, K. A. Hirsch, P. Zhang and J. S. Moore, *J. Chem. Educ.*, 1997, **74**, 915; F. A. Cotton and G. Wilkinson, *Advanced Inorganic Chemistry*, 5th edn., Wiley, Chichester, 1988; L. Tei, V. Lippolis, A. J. Blake, P. A. Cooke and M. Schröder, *Chem. Commun.*, 1998, 2633.

16 (*a*) L. Carlucci, G. Ciani, D. M. Proserpio and A. Sironi, *J. Am. Chem. Soc.*, 1995, **117**, 4562; (*b*) D. Venkataraman, S. Lee, J. S. Moore, P. Zhang, K. A. Hirsch, G. B. Gardner, A. C. Covey and C. L. Prentice, *Chem. Mater.*, 1996, **8**, 2030.

17 R. G. Vranka and E. L. Amma, *Inorg. Chem.*, 1966, **5**, 1020.

18 A. J. Blake, N. R. Champness, M. Crew and S. Parsons, *New J. Chem.*, 1999, **23**, 13.

19 L. D. Ciana and A. Haim, *J. Heterocycl. Chem.*, 1984, **21**, 607.

20 N. R. Champness, A. N. Khlobystov, A. G. Majuga, M. Schröder and N. V. Zyk, *Tetrahedron Lett.*, 1999, **40**, 5413.

21 E. F. Lier, S. Hunig and H. Quast, *Angew. Chem.*, *Int. Ed. Engl.*, 1968, **7**, 814.

22 S. Hunig, J. Grob, E. F. Lier and H. Quast, *Liebigs Ann. Chem.*, 1973, 355.

23 J. Cosier and A. M. Glazer, *J. Appl. Crystallogr.*, 1986, **19**, 105.

24 G. M. Sheldrick, SHELXS 97, University of Göttingen, 1997.

25 G. M. Sheldrick, SHELXL 97, University of Göttingen, 1997.